

Contents lists available at ScienceDirect

Fuel

journal homepage: www.elsevier.com/locate/fuel



Full Length Article

Development of silicon quantum dots based nano-fluid for enhanced oil recovery in tight Bakken cores



Yanxia Zhou^{a,b,c}, Xu Wu^a, Xun Zhong^d, Shaojie Zhang^d, Hui Pu^{d,*}, Julia Xiaojun Zhao^{a,*}

- ^a Department of Chemistry, University of North Dakota, Grand Forks, ND 58202, USA
- ^b College of Petroleum Engineering, Northeast Petroleum University, Daqing, Heilongjiang 163318, China
- c Key Laboratory of Enhanced Oil Recovery of Education Ministry, Northeast Petroleum University, Daqing, Heilongjiang 163318, China
- ^d Department of Petroleum Engineering, University of North Dakota, Grand Forks, ND 58202, USA

ARTICLE INFO

Keywords:

Silicon quantum dots Nano-fluid Interfacial tension Oil contact angle Enhanced oil recovery

ABSTRACT

A novel silicon quantum dots (SiQDs) based nano-fluid was first developed for effectively recovering Bakken Oil. The Bakken Formation is one of the largest contiguous deposits of unconventional oil in the USA and Canada. However, the oil recovery rate is only 5%–10% due to the existence of abundant tiny pores and ultra-low permeability. In this work, a novel nano-fluid was developed using ultra-small sized silicon quantum dots (SiQDs) coated with a zwitterionic surfactant. The nano-fluid exhibited good stability in synthetic high salinity brine containing divalent cations at high temperature and excellent capabilities in reducing interfacial tension and altering wettability, making it a good enhanced oil recovery (EOR) agent for tight Bakken Formation. Experimental results showed that the developed nano-fluid recovered 25.72 %OOIP (original oil-in-place) from Bakken core samples by spontaneous imbibition, which was 7.49 %OOIP higher than using surfactant alone. Similar results were obtained in the core flooding tests, where 41.98 %OOIP was finally recovered by the nano-fluid, compared to 30.28% in surfactant case. Herein, the mechanisms of disjoining pressure and synergistic effects between surfactant and nanoparticles have also been put forward. In short, the developed quantum dots based nano-fluid has played an instructive and a reference role in the application of oil field and would be a potential oil displacing agent for EOR.

1. Introduction

The Bakken Formation is one of the largest contiguous deposits of oil and natural gas, occupying about 200,000 square miles (520,000 km²) of the subsurface of the Williston Basin with a mean estimate of 7.4 billion barrels of oil by the U.S. Geological Survey [1]. However, the oil flow is very difficult in the Bakken tight porous media [2] due to its very low porosity and low permeability. Thus, the Bakken field was considered a marginal to sub-marginal oil resource [3]. However, given the huge energy demand, the development of effective drilling methods for tight oil reservoirs is in great need. The good news is, since 2008, successful horizontal drilling and hydrofracturing have transformed the Bakken Formation into a prolific oil and natural gas producer [4,5].

Although the production of unconventional tight oil and gas reservoirs based on horizontal well and multi-stage fracturing technology has promoted the rapid growth of tight oil production, the recovery rate is still very low, only occupies 5%-10% of the originally oil in place

(OOIP) [6,7]. In order to effectively develop the residual tight oil, various EOR methods have been widely studied, such as water or surfactant injection [8,9], cyclic gas injection (mostly are carbon dioxide) with huff and puff mode or gas flooding mode [10,11], foam-based system application [12]. However, the enhanced oil recovery in the tight oil field remains challenging due to the low mobility of water or surfactant or gas [13], and gas channeling along the formation fractures [14], and excessive injection pressure in foam flooding damaging the formation in some degree [15].

With the development of nanomaterials, nano-fluids consisting of nanoparticles and bulk liquid have attracted great attention in EOR [16,17]. Some NPs in distilled water or low salinity water have showed promising performance for promoting oil recovery [18]. However, most of the nano-fluids studied in the past were unable to enter into the tiny pores of the tight formations due to the large particle size (~100 nm) [19–20], which greatly limits the application of nano-fluids in unconventional reservoirs with abundant nanopores (< 10 nm) and mesopores (~25 nm) [21]. So the development of novel nano-fluids with

E-mail addresses: hui.pu@und.edu (H. Pu), julia.zhao@und.edu (J.X. Zhao).

^{*} Corresponding authors.

smaller nanoparticles capable to enter into tiny pores is in need.

Quantum dots that are only a few nanometers in size have flourished in many fields, including single-electron transistors [22], LEDs [23], lasers [24], solar cells [25], quantum computing [26], and medical imaging [27], etc. However, up until now, quantum dots have not yet been investigated in the EOR field. Given its much smaller size than regular nanoparticles, the quantum dots can suspend more easily in solution and offer a larger interfacial area for modification or functionalization to improve its satiability. In consequence, the quantum dots based nano-fluid might be a good candidate for effectively developing tight formations.

Most of the developed nano-fluid can work under a low temperature and salinity through the researchers' efforts [28]. However, the formation brine salinity and temperature of actual oil reservoir are very high [29]. For example, the salinity of Bakken formation brine is up to 150,000-320,000 ppm and the temperature is up to 80-120 °C [30] in which conditions conventional nano-fluids are unstable and would aggregate [31]. Therefore, it is necessary to modify the conventional nano-fluids. In our previous work, a polymer nanoparticle based nanofluid (polyNP-fluid) with good stability at high temperature and salinity was developed [32]. However, its particle size was around 30 nm which was larger than the tiny pores of Middle Bakken tight formation with average pore size of around a dozen nanometers [9]. The previous polyNP-fluid was targeting Berea sandstone that has large pores and it cannot be used to Bakken formation. To target Bakken formation with very small pores, it is necessary to develop a new nano-fluid able to enter the Bakken porous structure with smaller particle size to recover the oil firmly locked inside. Also in our pervious work, Berea core samples were used in the performance evaluation of the polyNP-fluid and core flooding experiment. To investigate the interface property and the recovering oil mechanism of nano-fluid for tight Bakken formation, it is also necessary to carry out the corresponding test using Bakken core sample for the newly developed nana-fluid.

Herein to enter into the tiny pores of Bakken formation and under the guidance of preparing nanofluid resistant temperature and salinity in our pervious polyNP-fluid work, a quantum dots based nano-fluid with smaller size and good stability was first developed in this paper. Thus positively charged silicon quantum dots (SiQDs) were coated by a zwitterionic surfactant *via* electrostatic force. The SiQDs based nanofluid showed improved stability in 15 wt% synthetic brine containing divalent cations at 80 °C. Both the static imbibition test and dynamic core flooding experiment in Bakken core samples show that the developed nano-fluid has a great potential to recover significant amount of additional oil. Considering the difficulty level of Bakken EOR and the huge amount of Oil in Bakken formation, this work would be very useful for Bakken formation.

2. Experimental section

2.1. Materials

Sodium L-ascorbate (SA, $\geq 99.0\%$) was purchased from Sigma-Aldrich. 3-Aminopropyltriethoxysilane (APTES) was purchased from Thermo Scientific. N-Alkyl-betaine (n = 12) surfactant were purchased from the Lubrizol Co. Sodium chloride (analytical grade, $\geq 99.5\%$), calcium chloride (analytical grade, $\geq 99.5\%$) and potassium chloride (analytical grade, $\geq 99.5\%$) were all purchased from VWR Chemicals and were used to prepare synthetic brine solution. The density and dynamic viscosity of Bakken crude oil were 0.82 g/cm³ at 20 °C and 2.28 mPa·s at 50 °C, separately. The Middle Bakken core samples were taken from Sanish Field in Mountrail County, ND. All the Bakken core plugs used were 2.54 cm in diameter, with porosity around 5% and permeability about $0.0091 \times 10^{-3} \ \mu m^2$.

2.2. Instruments

A high-resolution transmission electron microscope (HRTEM, JEOL JEM-2100) was used to observe the morphology and crystal structure of the silicon quantum dots. An energy-dispersive X-ray spectroscope (EDS, Oxford, X-Max) installed in the Hitachi SU8010 electron scanning microscope was used for elemental analysis. A spectrofluorophotometer (Shimadzu corporation, RF-6000) was used to determine the fluorescence properties of the silicon quantum dots. Zeta potential and particle size measurements were carried out based on the dynamic light scattering (DLS) using a Zeta sizer Nano Series (Malvern, Westborough). The infrared spectroscopy analysis was conducted using a Fourier transform infrared spectrometer (FT-IR, Spectrum ATR iD5). The interfacial tension and contact angle were measured using a Spinning Drop Tensionmeter (M6500, Grace Instrument Company) and Interfacial Tension Cell Model (IFT-10, ramé-hart instrument co.) respectively. X-Ray diffractometer (XRD, Smartlab-3KW) was used to analyze the phase and the internal molecular information of the Bakken core sample powder which was grinded by Mixer/Mill (8000 M, SPEX Sample Prep) and Shatter Box (8530, SPEX Sample Prep). A scanning electron microscope (SEM, Quanta 650 FEG) was used to observe the surface morphology of a Bakken core sample. All core samples were saturated by Bakken crude oil with the vacuum saturation device (ZYB-II Type, Hai'an Huacheng Scientific Research Instrument Co., Ltd.). Imbibition cells (Allen Scientific Glass, Inc.) were used to hold the imbibition liquid and Bakken formation core samples. The assembled core flooding system (see Supporting Information Fig. S1) was used to test the potential of the surfactant and SiQDs based nano-fluid to recover additional oil. In the system, some equipment was set inside the oven (UF260, Wisconsim Oven Distributors, LLC) which was set at 80 °C, others were set outside. The equipment inside the oven include: a displacement fluid accumulator (37181-3987, Vinci Technologies), a core holder (37181, Vinci Technologies) and two pressure sensors (CV-310-HC, Vindum Engineering, Inc.). The equipment outside the oven include: a pump (BTSP125-20, FLOXLAB) for displacing the fluid accumulator and another pump (P391, Enerpac company) for confining pressure and pressure recording end (VS15453, ViewSonic).

2.3. Synthesis of silicon quantum dots (SiQDs)

The synthesis of SiQDs was based on a "green" one-step synthetic method [33]. 3-Aminopropyltriethoxysilane (APTES) was used as the Si source and sodium L-ascorbate (SA) was used as the reduction reagent to prepare SiQDs since SA has a higher reduction property [33–35]. Briefly, 2.0 mL of APTES and 2.5 mL of 0.1 M SA were mixed in 8.0 mL distilled water under fierce stirring (≥1200 rpm) at 37 °C for 4 h. Afterwards, excess chemical reagents including APTES and SA were removed by a centrifugal filter whose molecular weight cut-off equals 3 kDa of MWCO at 8000 rpm ultrafiltration for three times.

2.4. Preparation of SiQDs based nano-fluid

The SiQDs based nano-fluid was prepared by adding different amounts of SiQDs into the betaine surfactant solution, and then the mixture was dissolved in synthetic brine. Prior to the preparation, the optimal concentration of betaine was determined, which was around its critical micelle concentration (CMC, 0.068 wt%, see Supporting Information Fig. S2). Therefore, the concentration of surfactant betaine is selected to be 0.1 wt%, which was slightly higher than the CMC considering its adsorption loss onto the reservoir rock surfaces. The method to determine the optimal concentration of surfactant is different from our pervious work of polyNP-fluid [32]. To prepare the nano-fluid, first, the pH value of the synthesized SiQDs was adjusted to be 7.0 (Effect of pH value on zeta potential of SiQDs see Supporting Information Fig. S3) because the pH value of most reservoir formations are around this value. Second, the surfactant betaine was added into

different concentrations of SiQD solutions (pH = 7.0). After 2 h of magnetic stirring and 2 h of ultrasonication, the surfactant molecules would adsorb onto the surface of SiQDs via electrostatic force. Then, the nano-fluid was diluted by synthetic brine to obtain the desired EOR fluid for further testing and injection [36-38]. It should be noted that our previous work of polyNP-fluid did not consider the effect of pH value in preparation of nano-fluid [32].

2.5. Interfacial tension measurement

The interfacial tension between Bakken oil and the oil displacing agents including surfactant and nano-fluid was tested using the spinning drop method [39]. In this method, a horizontally arranged capillary filled with the target solution to be tested and a specifically lighter oil drop phase suspended in the center of solution were set in rotation. The diameter or curvature of the drop which is elongated by centrifugal force correlates with the interfacial tension. In order to minimize the error caused by the curvature of the interface, the length of the drop along the axis of rotation must be between four to six times of the drop diameter. Then the interfacial tension can be calculated from the measured drop diameter at a given rotation speed when the densities of the two phases (oil and solution) are known. All measurements were repeated for three times. It should be noted that the inverted pendant method was used to measure the interfacial tension in our previous work of polyNP-fluid [32], which is different from this one.

2.6. Thermal stability of the SiQDs based nano-fluid

A bottle of 10.0 mL of the nano-fluid was placed in an oven at a constant temperature of 80 °C for 30 days. In order to determine whether the nano-fluid is stable or not, the size and the interfacial tension of the nano-fluid were tested every 5 days. The above-described nanoparticle size and interfacial tension measurements (see Section 2.5) were applied to this test. It should be noted that our previous work of polyNP-fluid did not consider the variation of interfacial tension at high temperature [32].

2.7. Oil contact angle measurement

The oil contact angle between the Bakken oil and the Bakken core sample slide in the nano-fluid was determined using the sessile drop method. However, the Berea core sample slide was used in our previous work of polyNP-fluid [32]. In this work, the Bakken sample slides were prepared with a diameter of ~ 0.5 cm and a length of ~ 0.1 cm for contact angle measurement. Prior to the test, these sample slides were aged in Bakken oil at 80 °C and atmospheric pressure for 10 days. The oil contact angle measure procedures are as following. First, the Bakken core sample slide was stuck onto a handle and inserted from the top of the chamber. The chamber was equipped with O-rings for sealing at each connection. Some electrical resistance wires were placed around the chamber for controlling the temperature of tested fluids. At the lower middle part of the chamber, there is an entrance to pump the tested fluid. After the tested fluid was pumped into the chamber, the inlet was closed. At the bottom of the chamber, there is an entrance to pump the Bakken oil. When the Bakken oil was pumped inside, a pendant oil drop was formed onto the Bakken core sample slide. At right side of the chamber, there is a high resolution camera centered at the middle position of the chamber. The oil droplet was captured on the oil-wet surface of Bakken core sample slide in a bulk nano-fluid phase at 80 °C by the camera. The contact angle was obtained from the image of the oil drop using a drop shape analysis by a Drop Image software (Finn Knut Hansen under an exclusive agreement with ramé-hart instrument company). All measurements were repeated for three times.

2.8. XRD analysis of Bakken core samples

The XRD analysis of Bakken core samples was conducted on crushed rock powders (< 270 mesh). First, the Bakken core chips were grinded in the Mixer/Mill for 5 min to reduce their size to < 1 to 2 mm. Then, about 2 g of the obtained coarse grinds were transferred to the steel container of Shatter Box for 5 min of grinding. After grinding, the powders should be sieved through the 270 mesh sieve. The ultimate quality diffraction data of minerals were obtained by analyzing those sieved powder. It should be noted that our previous work of polyNP-fluid did not analyze the mineral composition of core samples [32].

2.9. Spontaneous imbibition tests

The Bakken core samples were first cleaned with toluene and methanol using distillation methods to remove organic contaminants and any adsorbed materials. Then the cleaned core samples were dried at 80 °C in the oven for 48 h, and their dry weights were measured after they were cooled down to room temperature and stored in a desiccator. A vacuum pump is needed to saturate oil for core samples. However, vacuum pumps that are used in laboratories usually are not sufficient enough. In order to fully saturate the Bakken cores with oil, these core samples were vacuumed and then saturated with carbon dioxide to eliminate the air inside. Lastly the core samples were vacuumed to remove the carbon dioxide and saturated with Bakken crude oil. By this stage, the Bakken core samples were fully saturated with oil. To make the oil saturated core samples oil-wet, the samples were aged in Bakken crude oil for about 20 days at 80 °C at atmospheric pressure.

Prior to the imbibition test, the oil saturated Bakken core samples were sealed and stored in Bakken oil at 80 °C. After the core sample was taken out, the oil droplets on the surface were removed and the cores were weighed. The weight difference before and after oil saturation determined the OOIP. To compare the oil recovery efficiency at 80 °C, three types of treating fluids were prepared as controls of the SiQDs based nano-fluid, including 15 wt% synthetic brine, 0.1 wt% betaine solution, and the SiQDs solution. The oil volume recovered from the Bakken core samples was recorded versus time. The imbibition tests were repeated using the core samples from the same well at the same depth. So the obtained data was convinced. It should be noted that our previous work of polyNP-fluid did not carry out spontaneous imbibitions test [32].

2.10. Core flooding tests

Same oil-saturated Bakken core samples were obtained according to the procedures in section 2.9. Then the cylindrical core samples were fitted in a Viton sleeve and inserted into the core holder and then confined under a confining stress of 20 MPa at 80 °C. The displacement fluids in accumulators were injected into core plugs in core holder to displace the oil. The pore volume (PV) was determined by sample bulk volume multiplied by its porosity. The core flooding experimental program was carried out as follows: conducting a 0.5 PV synthetic brine flooding; then a 0.5 PV chemical flooding and finally followed by a 0.5 PV subsequently synthetic brine flooding at a constant flow rate of 0.1 mL/min at 80 °C. The volume of produced oil and water, and the pressure difference between the injection end and the production end of the core sample were recorded. The core flooding tests were repeated using the core samples from the same well at the same depth. So the obtained data was convinced.

3. Results and discussions

3.1. The design of SiQDs-Surfactant based Nano-fluid

The schematic diagram of the designed SiQDs-surfactant based nano-fluidis was shown in Fig. 1. The quantum dots with much smaller

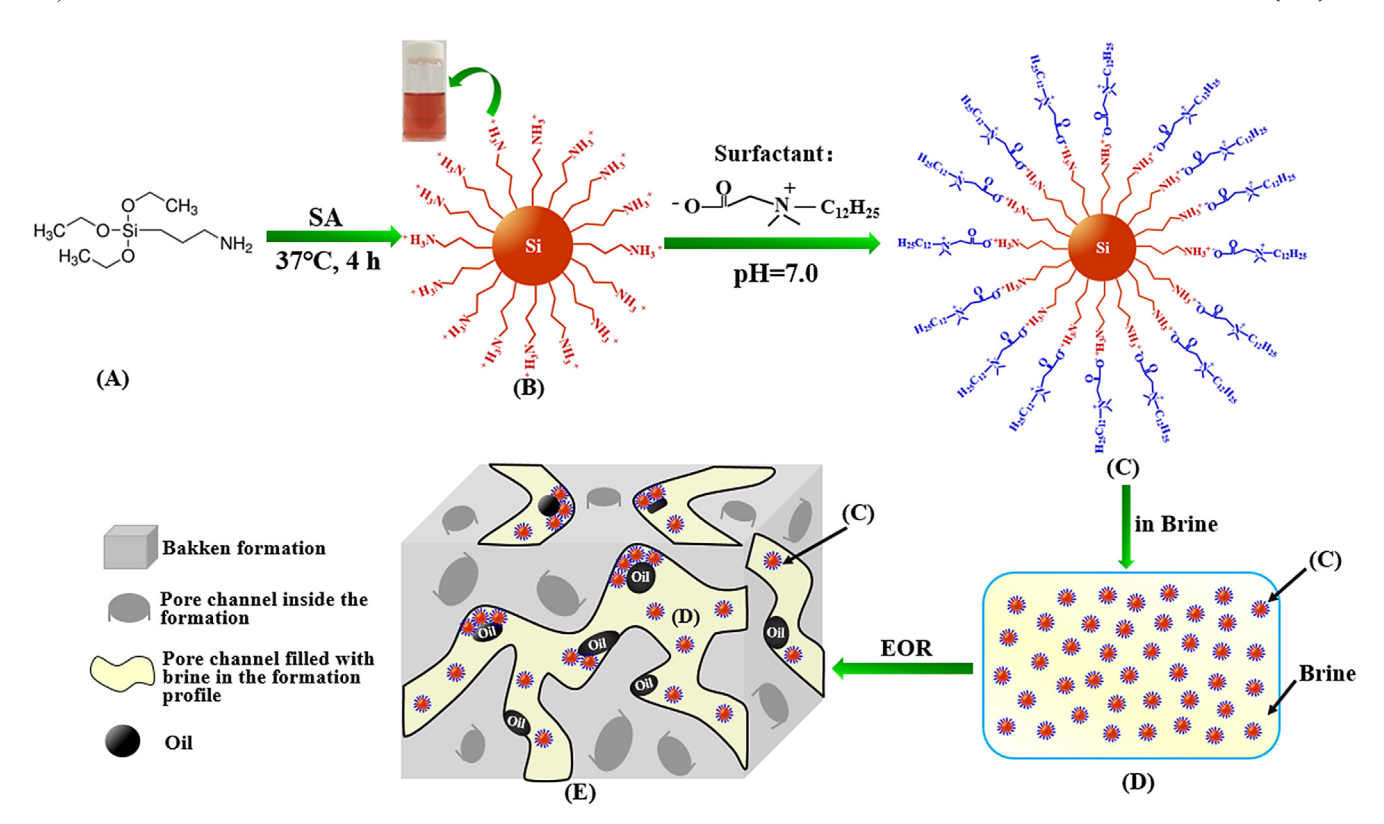


Fig. 1. Schematic diagram of the designed nano-fluid. (A) APTES. (B) SiQDs. (C) SiQDs-augmented surfactant nano-composite. (D) Nano-fluid prepared by synthetic brine. (E) The application of the nano-fluid on Bakken formation to recover oil.

size than regular nanoparticles may be a good candidate for preparing an EOR agent for tight formations with abundant tiny pores and pore throats. The nano-fluid consists of nanoparticles already proved to have great potential in EOR field as long as it is stable under reservoir conditions. In this paper, the QDs based nano-fluid with high tolerance towards temperature and salinity was employed to recover oil from the Bakken tight formation. First, APTES (Fig. 1A) was reduced to form SiQDs (Fig. 1B) under the catalysis of SA. Then the SiQDs became positive charge at pH 7.0 and thus attracted the surfactant molecules to its surface (Fig. 1C), forming a SiQDs-augmented surfactant nano-composite. Afterwards, the nano-composite was dissolved in a 15 wt% synthetic brine to form the nano-fluid (Fig. 1D). Finally, the nano-fluid was employed on Bakken core samples to test its EOR capability (Fig. 1E).

The SiQDs were selected as a carrier due to its several important features. First, their small size of no more than 5 nm allow them easily to enter into the tiny pores of Middle Bakken tight formation with average pore size of around 10–26 nm [40]. Second, a high yield rate for SiQDs (1 mL of APTES can produce 0.1 g of SiQDs [28]) makes it possible to scale up for oil field application. Third, the low toxicity of SiQDs was the most attractive aspect for its application in the oil production while other quantum dots often are toxic due to containing heavy metal elements, such as cadmium (Cd) [41]. Therefore, the SiQDs were selected for making the nano-fluid.

The linkage of surfactants to SiQDs could be achieved through both covalent attachment and adsorption [42,43]. However, the chemical covalent attachments require complicated processes, including the control of reaction temperature and time, separation and extraction of reactants, etc., also, the reaction process is difficult to control due to the occurrence of side reactions [44]. In contract, there is no cumbersome synthetic steps in physical adsorption methods, in which electrostatic force is a common linking force [45]. In our previous works, the electrostatic adsorption has been successfully used for nanoparticles with surfactants [32,46]. Therefore, the surfactant coated SiQDs *via* the electrostatic force was performed in this work. Due to the surface of the

SiQDs containing positively charged amino groups (Fig. 1B), the negative end of the zwitterionic surfactants were then coated onto the surface of SiQDs *via* electrostatic force (Fig. 1C), therefore, forming the SiQDs-augmented surfactant nano-composition.

Stable and applicable nano-fluids as an EOR agents were proved advantageous for oil recovery [47,48]. Therefore, the SiQDs based nano-fluid formed by the nano-composite in synthetic brine was kept at 80 °C for an extended time to test its thermal stability. Two crucial parameters including interfacial tension and contact angle were both measured. At last, the spontaneous imbibition and core flooding experiments were conducted to test its potential of recovering oil from the Bakken core samples.

3.2. Characterization of the SiQDs and the SiQDs-augmented surfactant nano-composite

The synthesized SiQDs were characterized regarding their morphology, size, fluorescence property, elemental composition, surface functional groups, and surface charge. The HRTEM image of the SiQDs is shown in Fig. 2A, which reveals the high crystallinity of the SiQDs. The QDs' lattice space was accurately measured to be 0.30 nm in the HRTEM image. The obtained quantum dots were in near spherical shape with a diameter of ca. 2.2 nm. The size and the size distribution were further characterized using a nanoparticle size analyzer as described in section 2.2. The obtained hydrodynamic diameter of the SiQDs and its distribution is shown in Fig. 2B with an average size of 2.8 \pm 0.4 nm that is comparable with the size obtained from the HRTEM image.

Quantum dots usually show fluorescence property. In this application, the fluorescence property of the QDs is not needed. However, to further confirm the formation of the QDs, we investigated their fluorescence property with distilled water as control. The fluorescence emission spectrum is shown in Fig. 2C with an emission peak of 512 nm at the excitation of 385 nm. The result confirmed that the obtained

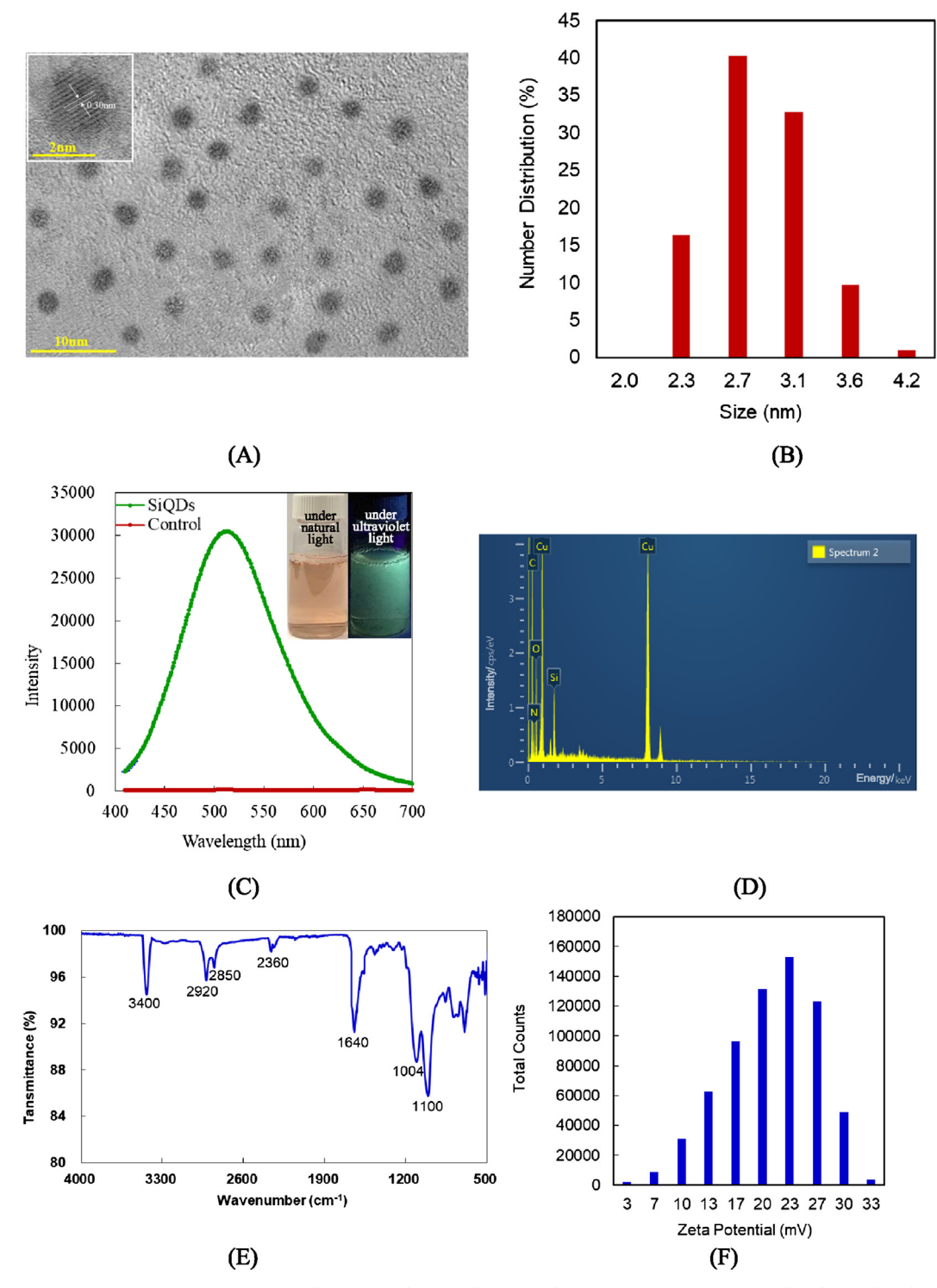


Fig. 2. Characterization of SiQDs. (A) A HRTEM image of the SiQDs with an acceleration voltage of 200 kV. (B) SiQDs size distribution based on the DLS method in distilled water at room temperature. (C) The fluorescence spectra of SiQDs @ 2 mg/ml with 10.0 nm of ex bandwidth at the excitation of 385 nm in distill water at room temperature with the control of distilled water. (D) EDS of the SiQDs. (E) The FTIR spectrum of SiQDs. (F) Zeta potential distribution of the SiQDs in distilled water (adjusting the pH value of the solution to 7.0 with 1 mol/L HCl) at room temperature.

material was quantum dots.

The elemental composition of SiQDs was analyzed using EDS (Fig. 2D). The result indicated the presence of silicon, oxygen, carbon, and copper, where the copper element was from the sample holder.

The functional groups on the QDs were confirmed by the FTIR analysis (Fig. 2E). The synthesized SiQDs were dried at 60 $^{\circ}\text{C}$ to obtain the SiQDs powder prior to the FTIR analysis. Theoretically, a sharp peak around 3400 cm $^{-1}$ on the FTIR spectrum is ascribed to $-\text{NH}_2$ group

[49–51]. In addition, a peak observed at $1640~\rm cm^{-1}$ was considered as the –NH $_2$ groups bending vibration. Two peaks at $1004~\rm and~1100~\rm cm^{-1}$ were ascribed to the group of Si–O–Si anti-symmetric stretching vibration [49–51] while a peak at $2360~\rm cm^{-1}$ was ascribed to the –Si–H stretching vibrations. The two peaks at $2920~\rm and~2850~\rm cm^{-1}$ were ascribed to the –CH $_2$ – stretching. The FTIR results confirmed the existence of amino groups on the SiQDs surface.

To further investigate the charges of the amino groups on the QDs

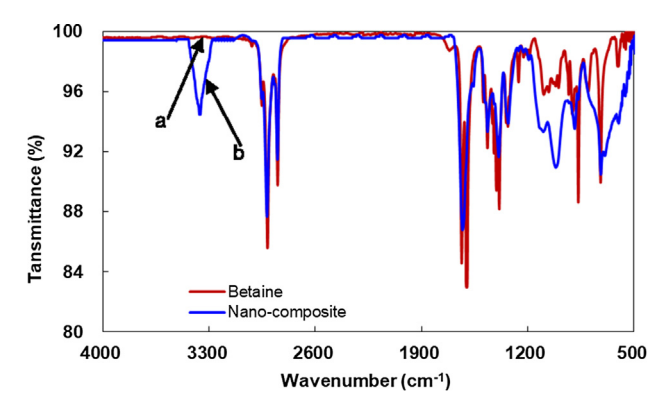


Fig. 3. FTIR spectra of the SiQDs-augmented surfactant nano-composite. Curve a: control of betaine surfactant; Curve b: SiQDs-augmented surfactant nano-composite.

surface, the zeta potential of the SiQDs was measured. The zeta potential of the SiQDs in distilled water (pH = 7.0) and its distribution is shown in Fig. 2F with an average value of + 23.2 \pm 0.6 mV. Based on this result, the amino groups were positively charged and therefore considered to be NH $_3$ ⁺.

The negatively charged end of betaine surfactant was used to adsorb onto the QDs to form the nano-composite. The characterization of the nano-composite was carried out using FTIR spectroscopy. First, the betaine surfactant solution used as the control was analyzed as shown in Fig. 3 curve (a). The peaks at 1600 cm⁻¹ and 1400 cm⁻¹ were associated to the vibration of carbonyl groups in carboxylates [49,50] and methyl stretching [52-53]. The peaks from 1250 cm⁻¹ to 1450 cm⁻¹ were ascribed to the stretching of -CH₃ group and C-O group. The two peaks at 2925 cm⁻¹ and 2850 cm⁻¹ were considered as -CH₂stretching. These characteristic groups partially proved the presence of betaine surfactant molecules. Then the surfactant functionalized nanoparticle-augmented nano-composites were characterized by FTIR (Fig. 3 curve (b)). All functional groups of betaine surfactant appeared on the spectrum, indicating the surfactant molecules have been successfully adsorbed on the QDs. In addition, a sharp peak appeared at $3300-3500 \text{ cm}^{-1}$, indicating the presence of -NH₂.

3.3. Evaluation of SiQDs based nano-fluid for EOR potential

3.3.1. Salinity resistance of the nano-Fluid

The salinity resistance is a necessary requirement for nano-fluid to be applied in oil fields especially in the high salinity reservoirs. However, most of the nano-fluids will easily agglomerate in high salinity conditions. To overcome this problem, in this design, we used surfactant to cover nanoparticles to avoid aggregation. The salt tolerance capability of the nano-composites in synthetic brine was tested through measuring the size of the nano-fluid ensured. The composition of synthetic brine was chosen according to the ratios of main ions in the Bakken formation water (see Supporting Information Table S1). Prior to the test, the concentrations of each component in the nano-fluid was determined. When the concentration of SiODs was higher than 0.3 wt% with the 0.1 wt% constant concentration of betaine, there were some precipitations at the bottom of the vial (see Supporting Information Fig. S4). This is mainly because a certain concentration of surfactant can only modify a certain number of nanoparticles, and excessive nanoparticles will precipitate in brine. Therefore, the concentration of SiQDs must be lower than 0.3 wt% and was determined to be a middle region value of 0.1 wt% in the nano-fluid size measurement. As shown in Fig. 4, the size of nano-fluid changed insignificantly when the salinity of synthetic brine increased from DI water to 15 wt% and the student t-test showed no significant difference, indicating electrostatic force between SiQDs and surfactant can counteract Brownian motion of anions and cations in the synthetic brine. However, when the salinity increased to

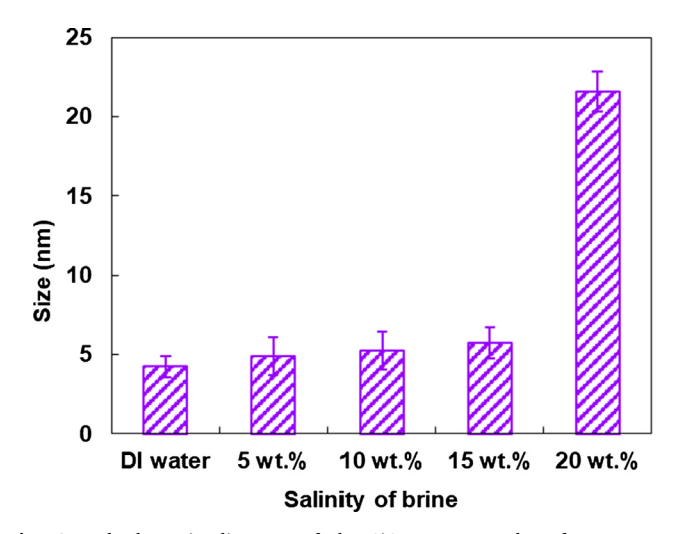


Fig. 4. Hydrodynamic diameter of the SiQDs-augmented surfactant nanocomposite with the $0.1~\rm wt\%$ concentration of both betaine and SiQDs in synthetic brine at room temperature.

20 wt%, the size increased greatly, indicating Brownian motion of a large number of anions and cations in simulated saline destroyed the electrostatic forces. Losing surfactant modification, the SiQDs became naked, which led to its aggregation. According to this, the highest salinity of the synthetic brine was determined to be 15 wt%. All the synthetic brines used in the following experiments are of the same salinity (15 wt%.) and composition (see Supporting Information Table S1).

3.3.2. Oil-brine interfacial tension measurement

An oil displacing agent with a lower oil–water interfacial tension (IFT) can reduce the residual oil saturation of the reservoir, which means an increment in the ratio of recoverable oil. The IFT between the Bakken oil and nano-fluid in the synthetic brine was measured with different concentration of SiQDs (Fig. 5). At the beginning the IFT of the pure betaine fluid without SiQDs was 0.83 mN/m (the IFT between the Bakken oil and the synthetic brine being 16.45 mN/m and not displayed in the Fig. 5). With the increment of SiQDs concentration, the IFT between Bakken oil and nano-fluid in the synthetic brine dropped rapidly.

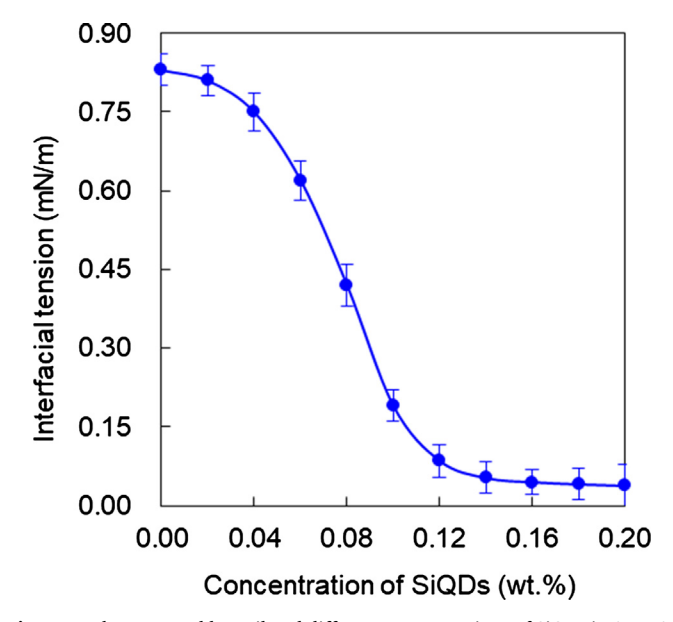


Fig. 5. IFT between Bakken oil and different concentrations of SiQDs in 15 wt% synthetic brine at 80 $^{\circ}$ C.

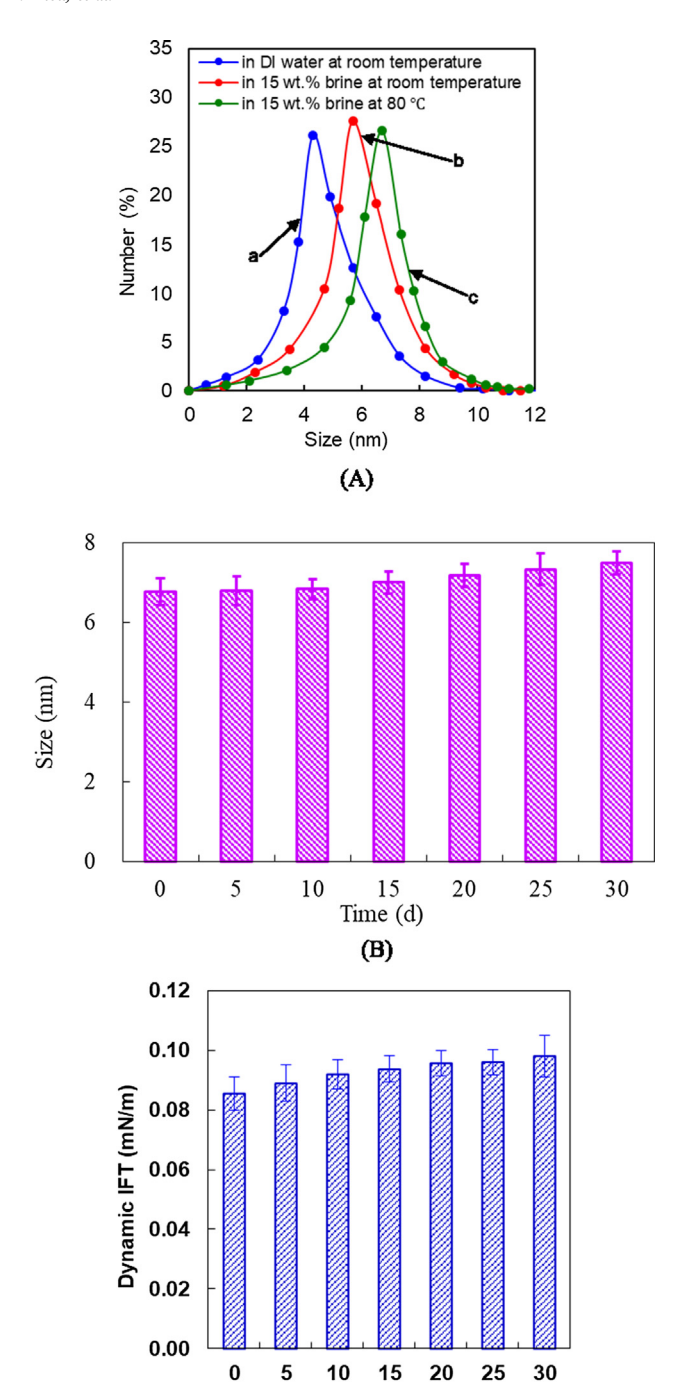


Fig. 6. Temperature resistance of SiQDs based nano-fluid. (A) The hydrodynamic diameter distribution after 1 day in DI water at room temperature (a); in 15 wt% synthetic brine at room temperature (b); and in 15 wt% synthetic brine at 80 °C (c). (B) The hydrodynamic dynamiter in 15 wt% synthetic brine at 80 °C for 30 days. (C) The interfacial tension between Bakken oil and nanofluid in 15 wt% synthetic brine at 80 °C for 30 days.

Time (d)

(C)

When the concentration of SiQDs was 0.12 wt%, the IFT reached 0.085 mN/m. The result showed that the nano-fluid reduced the IFT by 89.76% compared with the betaine surfactant solution. Beyond the 0.12 wt% of SiQDs concentration, the IFT appeared as a plateau. So, the concentration of SiQDs in the nano-fluid was higher than 0.12 wt% in the future oil displacement experiments.

3.3.3. Temperature resistance of the nano-fluid

Most nanoparticles are easy to agglomerate at high salinity and high temperature. The salinity of Bakken formation is up to 15–32 wt% and the reservoir temperature is in the range of $80-120\,^{\circ}\text{C}$. Therefore, the thermal stability of the designed nano-fluid was investigated prior to EOR application. In order to ensure that the nano-fluid can maintain its original properties at high temperatures, the size of nano-fluid and interfacial tension between Bakken oil and nano-fluid in the synthetic brine at high temperature were applied to determine its thermal resistance.

First the size distributions of the nano-fluid at different temperatures were tested, as shown in Fig. 6A. An average size of 4.3 \pm 1.1 nm was obtained in DI water at room temperature (Fig. 6A cure (a)). The particle size changed to 5.7 \pm 1.3 nm when in 15 wt% of the synthetic brine at room temperature for 24 h (Fig. 6A curve (b)). When the temperature increased to 80 °C in 15 wt% synthetic brine for 24 h (Fig. 6A curve (c)), the size changed to 6.7 \pm 1.5 nm. The results indicated that the high salinity and high temperature sped up the ion movement, resulted in more water molecules attached to the nanocomposite and thus increased their hydrodynamic diameter.

The hydrodynamic dynamiter of the nano-fluid was measured in 15 wt% synthetic brine at 80 °C for 30 days to evaluate the nano-fluid thermal stability (Fig. 6B). During the 30-day period, the size of the nano-fluid remained stable at about 7 nm, and the student *t*-test showed no significant difference of these data. The SiQDs-augmented surfactant nano-composite was stable at this temperature and salinity condition.

The interfacial tension between Bakken oil and nano-fluid was tested in 15 wt% synthetic brine at 80 °C for 30 days to further evaluate the nano-fluid thermal stability (Fig. 6C). During the 30-day period, the interfacial tension remained stable at about 0.085–0.098 mN/m, indicating the nano-fluid kept the initial ability to reduce interfacial tension. The nano-fluid was stable in 15 wt% synthetic brine at 80 °C, which was used as oil recovery conditions.

The SiQDs based nano-fluid remained stable in harsh conditions due to two factors. First, after the zwitterionic surfactant molecules adsorbed on the surface of SiQDs, hydrophobic groups of the surfactant produced a strong steric repulsion that stabilized the nano-fluid [32,46,54]. Second, the zwitterionic surfactant has a strong chelation interaction with divalent cations [55]. Therefore, this kind of nano-fluid kept its stability at high salinity and high temperature.

3.3.4. Oil-brine-rock contact angle measurement

Understanding reservoir wettability is crucial for optimizing oil recovery. In water wet formations, water can spread over a wide range of pores, and more crude oil on the surface of the reservoir formation could be extracted. However, most natural reservoirs are weak oil-wet or oil-wet. Therefore, changing the reservoir wettability from oil-wet to water-wet is beneficial for the prospective of oil recovery. The wettability could be characterized by measuring the contact angle of Bakken oil to the Bakken core sample slide in the tested solution. Thus, we tested the contact angles among Bakken oil, 15 wt% synthetic brine and Bakken rock at 80 °C. As shown in Fig. 7, when there was only betaine in synthetic brine, the original contact angle among Bakken oil, betaine surfactant solution and Bakken rock was 100.1° (the contact angle among oil/synthetic brine/Bakken core being 49.2° and not displayed in the Fig. 7). With the increment of SiQDs concentrations, the contact angle of nano-fluid to the rock increased slowly when its concentration was lower than 0.04 wt%. After that concentration, the contact angle increased rapidly and reached 124.1° when the SiQDs concentration reached 0.09 wt%. The contact angle then increased slowly and formed a plateau. Thus, the concentration of SiQDs in the nano-fluid was higher than 0.09 wt% in the future application of EOR experiments. Combined with the results of the previous interfacial tension measurements, the concentration of SiQDs was determined as 0.12 wt%.

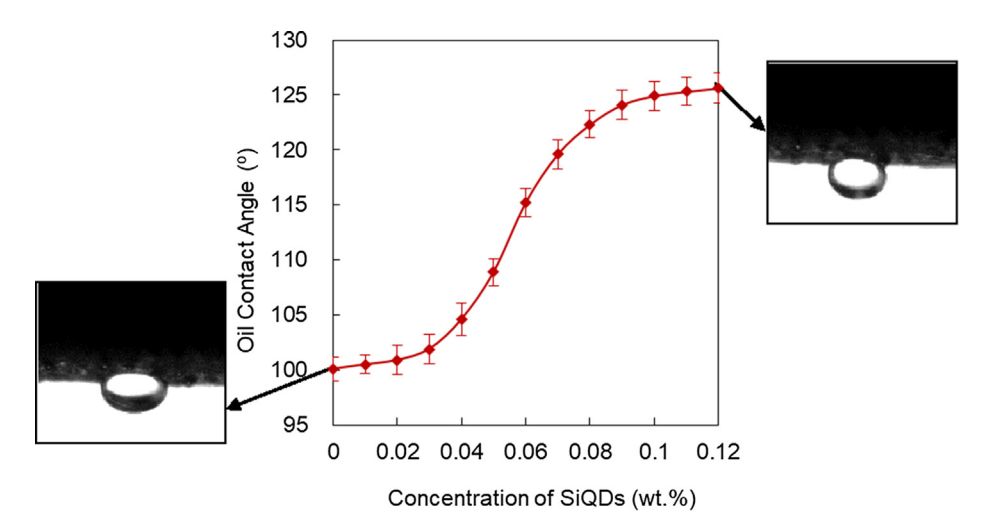


Fig. 7. Contact angles among Bakken oil, SiQDs based nano-fluid and Bakken rock slide at 80 °C.

3.4. Application of EOR using the nano-fluid

3.4.1. Bakken core sample analysis

Prior to EOR application, the Bakken rock samples were analyzed regarding their porosity, permeability, and oil saturation. The results are shown in Table 1. The XRD method was applied to qualitatively analyze the Bakken core sample composition. The results showed that the quartz, calcite and dolomite were the main components, respectively occupying 52.3 \pm 4.0%, 24.6 \pm 2.0% and 16.4 \pm 3.0% in the Bakken cores samples. Among the remaining components, feldspar and illite respectively occupied 5.5 \pm 2.0% and 1.2 \pm 1.0%.

The pore size of the tight formation is very small to the point where crude oil cannot flow into them. Therefore, whether there are fractures in the formation is very important for oil production. Thus, the morphology of the cores was observed on the SEM images to check the presence of micro fractures (Fig. 8A). The images show that there are many fine fractures in the Bakken formation, which is beneficial for oil flow. The zoom in image of Fig. 8(B) indicates that most fine fracture channels in Bakken formation are around a few hundred nanometers, which are the main oil flowing channels. As a result, it is possible for SiQDs based nano-fluid to recover oil from Bakken core samples since the small particle sizes of nano-fluid allow it to enter the tiny pores and micro-fractures to mobilize the trapped oil.

3.4.2. Imbibition test

The evaluation of high salinity and thermal stability, IFT and contact angle of nano-fluid indicated that the SiQDs based nano-fluid had a potential to recover oil. The spontaneous imbibition test was carried out at 80 °C and atmospheric pressure. Three controls of SiQDs based nano-fluid were prepared including 15 wt% synthetic brine, SiQDs solution, and 0.1 wt% surfactant betaine. The oil recovery of the imbibition test and the repeated one were around the same range. So the obtained data was convinced. In one group of the imbibition tests, the final oil recoveries of 15 wt% synthetic brine (Fig. 9A cure (a)), bare SiQDs without surfactant (Fig. 9A cure (b)), and 0.1 wt% betaine without

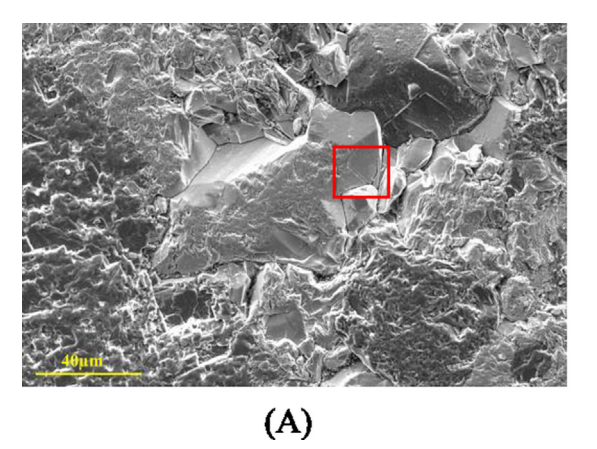
SiQDs (Fig. 9A cure (c)) were 12.33%, 8.68%, and 18.23% of OOIP, respectively. The SiQDs alone showed less oil recovery due to the instability of the bare QDs in high salinity condition (see Supporting Information Fig. S5). Particle aggregation and precipitation may block the pores [56]. The blocked pores hindered the flow of oil and imbibing fluid, which resulted in a lower oil recovery compared with the controls of 15 wt% synthetic brine. Finally, when the nano-fluid was used, and the oil recovery (Fig. 9A cure (d)) reached 25.72 %OOIP. This result indicated that the developed nano-fluid could be a beneficial oil displacement agent for EOR. With further analysis, the incremental oil recoveries of the control of 0.1 wt% betaine without SiQDs, the control of bare SiODs without surfactant and SiODs based nano-fluid is 5.90 % OOIP. -3.65 %OOIP and 13.39 %OOIP, respectively, compared to the control of 15 wt% synthetic brine. The enhanced oil recovery of the nano-fluid was much higher than that of the sum of betaine solution without SiQDs and bare SiQDs solution without surfactant, which indicated there was a synergistic effect between surfactant betaine and SiQDs. It should be noted that our previous work of polyNP-fluid did not put forward there was a synergistic effect between the surfactant and nanoparticles benefit oil recovery [32].

The imbibition rates of the nano-fluid and its controls were also analyzed as shown in Fig. 9B. The imbibition rate (%OOIP/d) at a certain time is the ratio of the oil recovery difference (%OOIP) between this time and the previous time to the time period (d), that is the average imbibition rate in this time period. One thing that needs to be clear is that the curve itself, not the slope of the curve, represents the imbibition rate. The imbibition rate in15 wt.% synthetic brine (Fig. 9B cure (a)) is slower than that in the SiQDs solution (Fig. 9B cure (b)) in the first day of imbibition and was faster than that in the SiQDs after the first day. Compared with the three controls (cure a, b, c), the imbibition rate in nano-fluid (Fig. 9B cure (d)) shows the highest velocity, and reaches a peak faster than other displacing fluids.

The above imbibition test showed that the nano-fluid yielded the best displacing effect and faster imbibition rate, which means a long effective production cycle and economic benefits respectively in the

Table 1 Properties of Bakken core samples.

| Sample | | Length, cm | Diameter, cm | Porosity, % | Permeability, $10^{-3}\ \mu\text{m}^2$ | Oil saturation, % |
|--------------------|----|------------|--------------|-------------|--|-------------------|
| Imbibition test | B1 | 3.52 | 3.81 | 5.3 | 0.0091 | 95.68 |
| | B2 | 3.47 | | 5.5 | 0.0092 | 96.54 |
| | В3 | 3.53 | | 5.1 | 0.0088 | 96.23 |
| | B4 | 3.49 | | 5.2 | 0.0090 | 95.84 |
| Core flooding test | C1 | 5.54 | | 5.4 | 0.0093 | 95.92 |
| | C2 | 5.61 | | 5.5 | 0.0091 | 96.43 |
| | | | | | | |



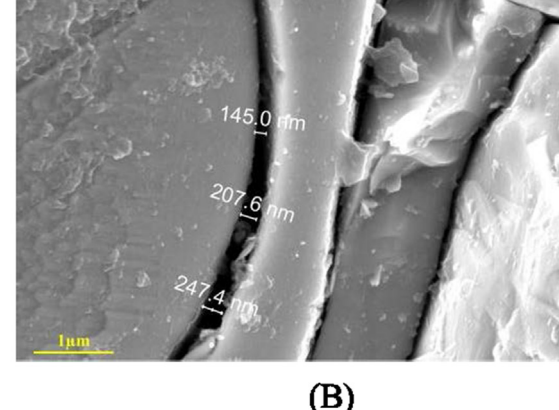


Fig. 8. (A) SEM images of Bakken formation core samples and (B) A zoom-in of the area outlined with red box with an acceleration voltage of 10.0 kV and working distance of 9.8 mm and no tilt of the sample. (For interpretation of the references to colour in this figure legend, the reader is referred to the web version of this article.)

actual oil field.

3.4.3. Core flooding test

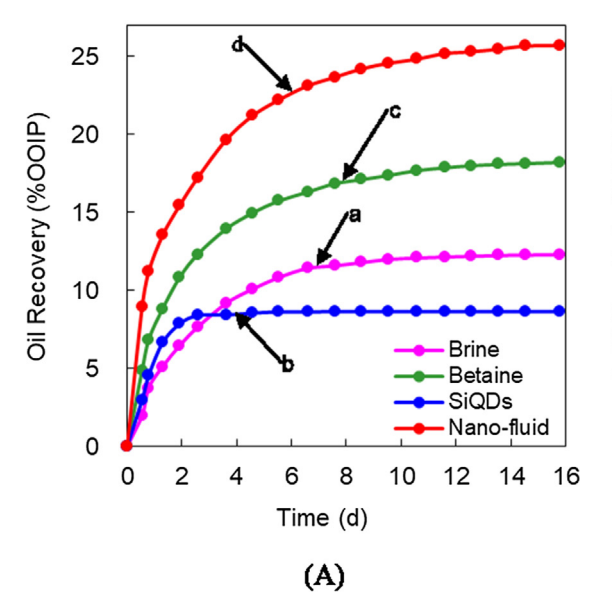
In order to simulate the injection and production process under formation pressure conditions, the core flooding test was carried out since the imbibition is a static process in atmospheric pressure environments. The betaine of 0.1 wt% was prepared as a control of the SiQDs based nano-fluid. The pure SiQDs solution was not used as a control because it is unstable at high salinity and temperature. The oil recovery of the core flooding test and the repeated one were around the same range. So the obtained data was convinced. In one group of the core flooding tests, the oil recoveries of different flooding are shown in Table 2. The water flooding recovery of the two Bakken core samples is 20.90 %OOIP and 21.18 %OOIP, respectively. In the chemical flooding stage, the oil recovery increased by 6.84 %OOIP by surfactant (betaine) flooding while the incremental oil recovery of nano-fluid is 15.97 % OOIP, which is 9.13 %OOIP higher than that of surfactant (betaine) flooding. Moreover, in subsequent brine flooding, compared with betaine flooding, nano-fluid flooding further increased oil recovery by 2.29 %OOIP. The results indicated that the SiQDs based nano-fluid recovered more oil and could be a potential oil displacing agent for EOR

Table 2
Oil recovery of core flooding test.

| Core samples | Type of chemical | Oil recovery(%OOIP) | | | | | |
|-----------------|------------------------|---------------------|-------------------|------------------------------|-------------------|--|--|
| | flooding | Brine flooding | Chemical flooding | Subsequent brine flooding | Total recovery | | |
| C1 | Betaine flooding | 20.90 | 6.84 | 2.54 | 30.28 | | |
| C2 | Nano-fluid flooding | 21.18 | 15.97 | 4.83 | 41.98 | | |

purpose.

Except the total recovery, the change of production index with the injection of the oil displacement agent, including the variation of oil recovery, the pressure difference and water-cut of produced liquid can also reveal its functional mechanisms. The oil recovery, pressure difference and water-cut of produced liquid with PV is shown in Fig. 10. During the first 0.5 PV brine flooding, the dynamic characteristic curves of oil recovery, pressure difference and water fraction with PV were very close, and almost identical. During the next 0.5 PV chemical



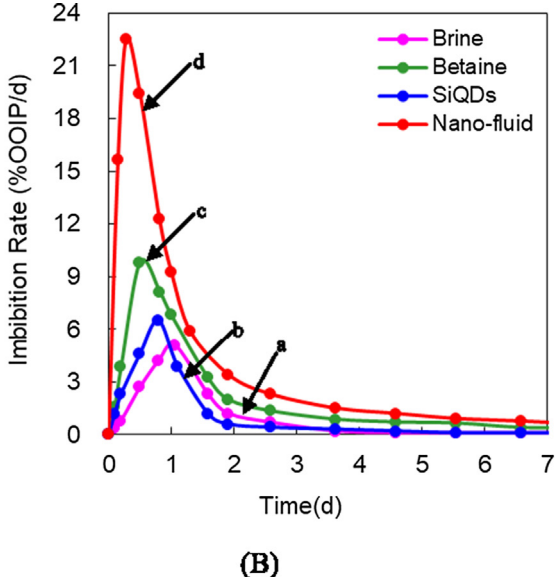


Fig. 9. Spontaneous imbibition experiments at 80 °C. (A) Oil recovery of different imbibition liquids in 16 d. Curve a: the control of 15 wt% synthetic brine. Curve b: the control of SiQDs solution. Curve c: the control of betaine solution. Curve d: the nano-fluid. (B) Imbibition rate in different imbibition liquids in the first 7 days. Curve a: the control of 15 wt% synthetic brine. Curve b: the control of SiQDs solution. Curve c: the control of betaine solution. Curve d: the nano-fluid.

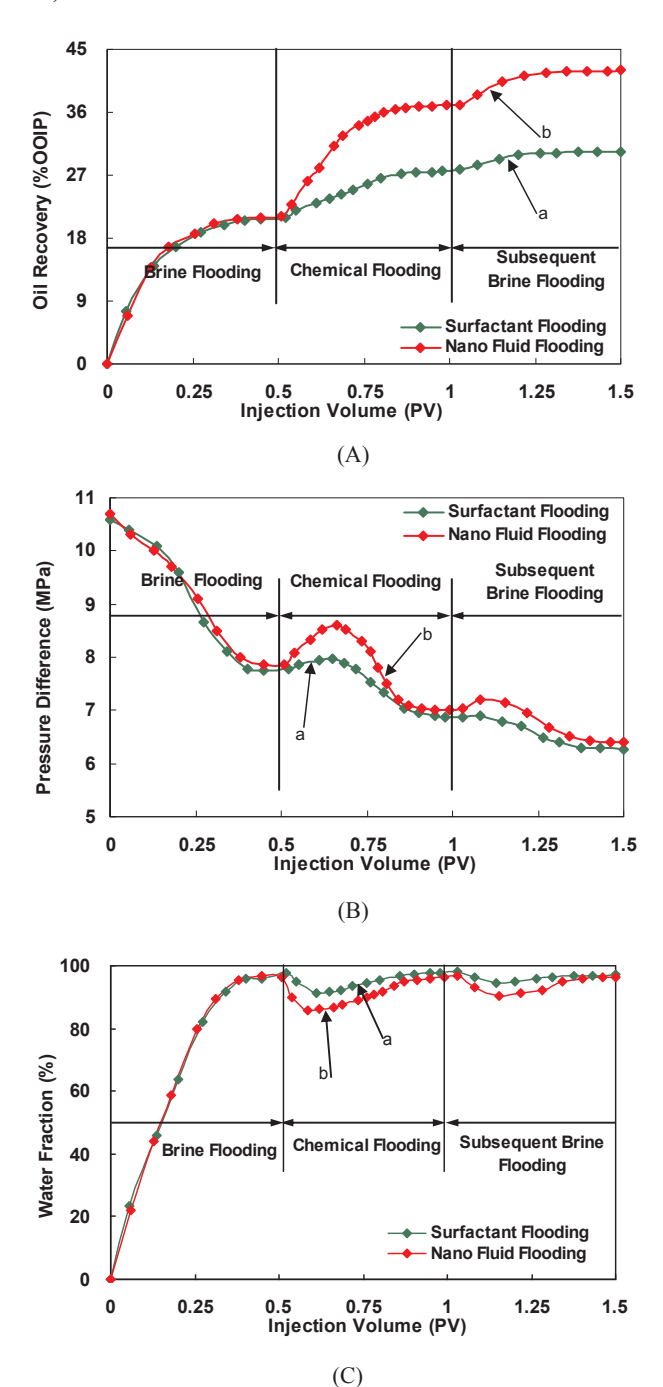


Fig. 10. Dynamic production curve of Bakken core sample at 80 °C. (A) Oil recovery of surfactant betaine flooding (a); and SiQDs based nano-fluid flooding (b). (B) Pressure difference of surfactant betaine flooding (a); and SiQDs based nano-fluid flooding (b). (C) Water-cut of produced liquid of surfactant betaine flooding (a); and SiQDs based nano-fluid flooding (b).

flooding, the oil recovery (Fig. 10A cure (b)) and pressure difference (Fig. 10B cure (b)) of the nano-fluid were both much higher than those (Fig. 10A cure (a), Fig. 10B cure (a)) of betaine flooding which indicated the nano-fluid has a much higher potential to recover oil than the surfactant. The water fraction of nano-fluid flooding (Fig. 10C cure (b)) was reduced greater than the surfactant flooding (Fig. 10C cure (a)) which meant that the nano-fluid displaced more remaining oil than the surfactant. During the subsequent brine flooding, both the oil recovery and pressure difference trends slowed down, however, those of the nano-fluid flooding were still much higher than the surfactant because of nano-composition retained in the Bakken cores. The opposite trend

for water fraction of the production liquid appeared, that is the water fraction with nano-fluid flooding had a slower rising trend than with the surfactant flooding. Besides the reduced IFT and improved water wettability, the disjoining pressure and synergistic effect between the surfactant and nanoparticle were helpful in improving oil recovery. When adding SiQDs to the pure surfactant system, a wedge film would form in the oil/nano-fluid/rock confined three-phase contact region. NPs inside the wedge film tend to form more ordered structures in the confined region, that is to say the NPs would be self-structuring in the confined region. The wedge-shaped film of NPs within the structure provides excess pressure i.e., the disjoining pressure [57–59], which is high near the vertex and results in movement of the larger oil droplets. Compared with SiODs, nano-fluid enhanced the nano-composite dispersibility and stability, and prevented SiQDs agglomeration. Compared with the surfactant, the nano-fluid augmented the surface activity, which can get a lower interfacial tension and stronger water wettability. So under the synergistic effects between the surfactant and nanoparticles, the nano-fluid showed a better performance for oil recovery.

4. Conclusions

In order to effectively recover the Bakken tight oil, a SiQDs based nano-fluid was developed. The average hydrodynamic diameter of synthesized SiQDs was 2.8 \pm 0.4 nm. With very small size, high yield rate and positive charge, the SiQDs can be coated with different surfactants through covalent attachment and adsorption to prepare nanofluids. With a high thermal resistance in the synthetic brine of high salinity, the developed SiQDs based nano-fluid kept its size and IFT around its original value due to electrostatic force between SiQDs and surfactant can counteract Brownian motion of anions and cations in the synthetic brine. With reduced IFT and improved water wettability which were favorable for oil recovery, the developed SiODs based nanofluid was applied to recover the oil in Bakken core samples. The results showed that after the nano-fluid was applied to recover Bakken oil in Bakken core samples, 25.72 %OOIP was recovered in spontaneous imbibition, which was 7.49 %OOIP higher than that of the surfactant betaine solution. The imbibition test also showed that the developed nano-fluid had a faster imbibition rate and a long effective production cycle. A total recovery of 41.98 %OOIP in core flooding test was achieved. The result was 9.13 %OOIP and 2.29 %OOIP higher than the surfactant in the chemical and subsequent brine flooding stages, respectively. Both the disjoining pressure and synergistic effect between the surfactant and nanoparticles benefit oil recovery. With good stability at both high temperature and high salinity, the developed nanofluid demonstrates a potential in the application of oil field.

Declaration of competing interests

The authors declare that they have no known competing financial interests or personal relationships that could have appeared to influence the work reported in this paper.

CRediT authorship contribution statement

Yanxia Zhou: Methodology, Data curation, Writing - original draft, Writing - review & editing. Xu Wu: Conceptualization. Xun Zhong: Formal analysis. Shaojie Zhang: Investigation. Hui Pu: Writing - review & editing, Supervision. Julia Xiaojun Zhao: Writing - review & editing, Supervision.

Acknowledgment

This work was supported by the North Dakota Industrial Commission Oil and Gas Research Program (Contract No.: G-041-081), the NSF grant CHE 1709160, UND Vice President for Research &

Economic Development Postdoctoral Funding Program. The authors acknowledge the use of the Edward C. Carlson Imaging and Image Analysis Core Facility which is supported in part by NIH grant 1P30GM103329. We are very grateful to Sarah Reagen, department of chemistry, University of North Dakota, for editing this paper and Xiaodong Hou, institute of energy studies, University of North Dakota, for helping data analysis of XRD.

Appendix A. Supplementary data

Supplementary data to this article can be found online at https://doi.org/10.1016/j.fuel.2020.118203.

References

- US Department of the Interior, "USGS releases new oil and gas assessment for Bakken and Three Forks", Press Release, Department of Interior. 4/30; 2013.
- [2] Zhang S, Li Y, Pu H. Studies of the storage and transport of water and oil in organicrich shale using vacuum imbibition method. Fuel 2020;266:117096.
- [3] Makinde I, Lee WJ. Forecasting Production of Shale Volatile Oil Reservoirs Using Simple Models. SPE/IAEE Hydrocarbon Economics and Evaluation Symposium, Houston, Texas, USA, 5/17-5/18; 2016.
- [4] Scanlon BR, Reedy RC, Male F, Hove M. Managing the increasing water footprint of hydraulic fracturing in the Bakken play, United States. Environ Sci Technol 2016;50(18):10273–81.
- [5] Strpić K, Miličević M, Kurevija T. Development of tight oil resources in the USA: exploitation costs and effect of macroeconomic indicators in a volatile oil price environment. Rudarsko Geolosko Naftni Zbornik 2017;32(3):23–33.
- [6] Song C, Yang D. Experimental and numerical evaluation of CO2 huff-n-puff processes in Bakken formation. Fuel 2017;190:145–62.
- [7] Xie K, Lu X, Pan H, Han D, Hu G, Zhang J, et al. Analysis of dynamic imbibition effect of surfactant in microcracks of reservoir at high temperature and low permeability. SPE 2018:33:596–606.
- [8] Qu X, Lei Q, He Y, Chen Z, Yu H. Experimental investigation of the EOR performances of carbonated water injection in tight sandstone oil reservoirs. IOP Conf Ser. Earth Environ Sci 2018;208:12054.
- [9] Zhang S, Pu H, Zhao JX. Experimental and numerical studies of spontaneous imbibition with different boundary conditions: case studies of middle Bakken and berea cores. Energy Fuels 2019;33:5135–46.
- [10] Zhang K, Qin T, Wu K, Jing G, Han J, Hong A, Zhang J, Chen S, Chen Z. Integrated method to screen tight oil reservoirs for CO2 flooding. SPE/CSUR Unconventional Resources Conference, Calgary, Alberta, Canada, 10/20-10/22; 2015.
- [11] Sheng JJ. Enhanced oil recovery in shale reservoirs by gas injection. J Nat Gas Sci Eng 2015;22:252–9.
- [12] Liu P, Zhang X, Wu Y, Li X. Enhanced oil recovery by air-foam flooding system in tight oil reservoirs: Study on the profile-controlling mechanisms. J Petrol Sci Eng 2017;150:208–16.
- [13] Ren G, Zhang H, Nguyen QP. Effect of surfactant partitioning between CO2 and water on CO2 mobility control in hydrocarbon reservoirs. SPE Enhanced Oil Recovery Conference, Kuala Lumpur, Malaysia. 7/19-7/21; 2011.
- [14] Duan X, Hou J, Zhao F, Ma Y, Zhang Z. Determination and controlling of gas channel in CO₂ immiscible flooding. J Energy Inst 2016;89(1):12–20.
- [15] Yu H, Yang B, Xu G, Wang J, Ren S, Lin W, Xiao L, Gao H. Air foam injection for IOR: from laboratory to field implementation in Zhongyuan Oilfield China. SPE Symposium on Improved Oil Recovery, Tulsa, Oklahoma, USA. 4/20-4/23; 2008.
- [16] Wei B, Li Q, Li H, Lu L, Pu W. Green EOR utilizing well-defined nano-cellulose based nano-fluids from flask to field. Abu Dhabi International Petroleum Exhibition & Conference, Abu Dhabi, UAE, 11/13-11/16; 2017.
- [17] Towler BF, Lehr HL, Austin SW, Bowthorpe B, Feldman JH, Forbis SK, et al. Spontaneous imbibition experiments of enhanced oil recovery with surfactants and complex nano-fluids. J Surfactants Deterg 2017;20(2):367–77.
- [18] Gomari SR, Omar YGD, Amrouche F, Islam M, Xu D. New insights into application of nanoparticles for water-based enhanced oil recovery in carbonate reservoirs. Colloids Surf, A 2019;568:164–72.
- [19] Nourafkan E, Hu Z, Wen D. Nanoparticle-enabled delivery of surfactants in porous media. J Colloid Interface Sci 2018;519:44–57.
- [20] Nwidee LN, Lebedev M, Barifcani A, Sarmadivaleh M, Iglauer S. Wettability alteration of oil-wet limestone using surfactant-nanoparticle formulation. J Colloid Interface Sci 2017;504:334–45.
- [21] Alharthy NS, Nguyen T, Teklu T, Kazemi H, Graves R. Multiphase Compositional Modeling in Small-Scale Pores of Unconventional Shale Reservoirs. SPE Annual Technical Conference and Exhibition, New Orleans, Louisiana, USA. 9/30-10/2; 2013
- [22] Ihn T, Güttinger J, Molitor F, Schnez S, Schurtenberger E, Jacobsen A, et al. Graphene single-electron ransistors. Materialstoday 2010;13(3):44–50.
- [23] Demir HV, Nizamoglu S, Erdem T, Mutlugun E, Gaponik N, Eychmüller A. Quantum dot integrated LEDs using photonic and excitonic color conversion. Nanotoday 2011;6(6):632–47.
- [24] Chen S, Li W, Wu J, Jiang Q, Tang M, Shutts S, et al. Electrically pumped continuous-wave III–V quantum dot lasers on silicon. Nat Photonics 2016;10:307–11.
- [25] Sargent EH. Colloidal quantum dot solar cells. Nat Photonics 2012;6:133–5.

[26] Veldhorst M, Hwang JCC, Yang CH, Leenstra AW, Ronde BD, Dehollain JP, et al. An addressable quantum dot qubit with fault-tolerant control-fidelity. Nat Nanotechnol 2014;9:981–5.

- [27] Liu Y, Ai K, Yuan Q, Lu L. Fluorescence-enhanced gadolinium-doped zinc oxide quantum dots for magnetic resonance and fluorescence imaging. Biomaterials 2011;32(4):1185–92.
- [28] Chen C, Wang S, Kadhum MJ, Harwell JH, Shiau BJ. Using carbonaceous nanoparticles as surfactant carrier in enhanced oil recovery: a laboratory study. Fuel 2018;222:561–8.
- [29] Aghaeifar Z, Strand S, Austad T, Puntervold T, Aksulu H, Navratil K, et al. Influence of formation water salinity/composition on the low-salinity enhanced oil recovery effect in high-temperature sandstone reservoirs. Energy Fuels 2015;29(8):4747–54.
- [30] Zhong X, Pu H, Zhou Y, Zhao JX. Comparative study on the static adsorption behavior of zwitterionic surfactants on minerals in middle Bakken formation. Energy Fuels 2019;33(2):1007–15.
- [31] Kim I, Taghavy A, DiCarlo D, Huh C. Aggregation of silica nanoparticles and its impact on particle mobility under high-salinity conditions. J Petrol Sci Eng 2015;133:376–83.
- [32] Zhou Y, Wu X, Zhong X, Reagen S, Zhang S, Sun W, et al. Polymer nanoparticles based nano-fluid for enhanced oil recovery at harsh formation conditions. Fuel 2020;267:117251.
- [33] Wang J, Ye D, Liang G, Chang J, Kong J, Chen J. One-step synthesis of waterdispersible silicon nanoparticles and their use in fluorescence lifetime imaging of living cells. J Mater Chem B 2014;2:4338–45.
- [34] Wang R, Zhao M, Deng D, Ye X, Zhang F, Chen H, et al. Intelligent and bio-compatible photosensitizer conjugated silicon quantum dots-MnO₂ nanosystem for fluorescence imaging-guided efficient photodynamic therapy. J Mater Chem B 2018;6:4592–5460.
- [35] Zhao Q, Zhang R, Ye D, Zhang S, Chen H, Kong J. Ratiometric fluorescent silicon quantum dots-Ce6 complex probe for the live cell imaging of highly reactive oxygen species. ACS Appl Mater Interfaces 2017;9:2052–8.
- [36] Thyne G, Brady P. Evaluation of formation water chemistry and scale prediction: Bakken Shale. Appl Geochem 2016;75:107–13.
- [37] Wang D, Butler R, Liu H, Ahmed S. Surfactant Formulation Study for Bakken Shale Imbibition. Paper SPE 145510 presented in 2011 SPE Annual Technical Conference and Exhibition held in Denver, Colorado, USA, 10/30-11/2; 2011.
- [38] Zhang J, Wang D, Butler R. Optimal Salinity Study to Support Surfactant Imbibition into the Bakken Shale. SPE 167142, presented at the SPE Unconventional Resources Conference-Canada held in Calgary, Alberta, Canada, 11/05–11/07; 2013.
- [39] Movsumova U. Investigation of interfacial tension of crude oils by spinning drop technique (Master Thesis) Leoben, Austria: University of Leoben; 2018.
- [40] Hawthorne SB, Jin L, Kurz BA, Miller DJ, Grabanski CB, Sorensen JA, Pekot LJ, Bosshart NW, Smith SA, Burton-Kelly ME, Heebink LV, Gorecki CD, Steadman EN, Harju JA. Integrating Petrographic and Petrophysical Analyses with CO2 Permeation and Oil Extraction and Recovery in the Bakken Tight Oil Formation. SPE Unconventional Resources Conference, Calgary, Alberta, Canada, 2/15-2/16; 2017.
- [41] Cheng X, Lowe SB, Reecec PJ, Gooding JJ. Colloidal silicon quantum dots: from preparation to the modification of self-assembled monolayers (SAMs) for bio-applications. R. Soc. Chem. 2014;43:2680–700.
- [42] Farahbakhsh F, Ahmadi M, Hekmatara SH, Sabet M, Heydari-Bafrooei E. Improvement of photocatalyst properties of magnetic NPs by new anionic surfactant. Mater Chem Phys 2019;224:279–85.
- [43] Heinz H, Pramanik C, Heinz O, Ding Y, Mishra RK, Marchon D, et al. Nanoparticle decoration with surfactants: Molecular interactions, assembly, and applications. Surf Sci Rep 2017;72(1):1–58.
- [44] Müller J, Bauer KN, Prozeller D, Simon J, Mailänder V, Wurm FR, et al. Coating nanoparticles with tunable surfactants facilitates control over the protein corona. Biomaterials 2017;115:1–8.
- [45] Hecht LL, Schoth A, Muñoz-Espí R, Javadi A, Köhler K, Miller R, et al. Determination of the ideal surfactant concentration in miniemulsion polymerization. Macromol Chem Phys 2013;214:812–23.
- [46] Zhou Y, Wu X, Zhong X, Sun W, Pu H, Zhao JX. Surfactant-Augmented functional silica nanoparticle based nanofluid for enhanced oil recovery at high temperature and salinity. ACS Appl Mater Interfaces 2019;11(49):45763–75.
- [47] Tarek M, El-Banbi AH. Comprehensive investigation of effects of nano-fluid mixtures to enhance oil recovery. SPE North Africa Technical Conference and Exhibition, Cairo, Egypt, 09/14-09/16; 2015.
- [48] Cheraghian G, Hendraningrat L. A review on applications of nanotechnology in the enhanced oil recovery part A: effects of nanoparticles on interfacial tension. Int Nano Lett 2016;2:129–38.
- [49] Kumar S, Rai SB. Spectroscopic studies of L-arginine molecule. Indian J Pure Appl Phys 2010;48:251–5.
- [50] Coates J. Interpretation of infrared spectra, A practical approach. Encyclopaedia Anal Chem 2000:10815–37.
- [51] Fvon Germar, Barth A, Mäntele W. Structural Changes of the Sarcoplasmic Reticulum Ca²⁺-ATPase upon nucleotide binding studied by Fourier transform infrared spectroscopy. Biophys J 2000;78:1531–40.
- [52] Nakanishi K, Solomon PH. Infrared Absorption Spectroscopy, 2nd ed. San Francisco: Holden-Day, 1977. QD95.N38. Characteristic IR Absorption Frequencies of Organic Functional Groups.
- [53] Silverstein RM, Bassler GC, Morrill TC. Spectrometric Identification of Organic Compounds 1981;QD272.S6:S55.
- [54] Li X, Qin Y, Liu C, Jiang S, Xiong L, Sun Q. Food Chem 2016;199:356–63.
 [55] Svanedal I, Boija S, Norgren M, Edlund H. Langmuir 2014;30(22):6331–8.
- [56] Sun X, Zhang Y, Chen G, Gai Z. Application of nanoparticles in enhanced oil

- recovery: a critical review of recent progress. Emeries 2017;10:345.

 [57] Chengara A, Nikolov AD, Wasan DT, Trokhymchuk A, Henderson D. J Colloid Interface Sci 2004;280:192–201.

 [58] Kondiparty K, Nikolov A, Wu S, Wasan D. Wetting and spreading of nanofluids on solid surfaces driven by the structural disjoining pressure: statics analysis and

- experiments. Langmuir 2011;27(7):3324–35.

 [59] Wasan D, Nikolov A, Kondiparty K. The wetting and spreading of nanofluids on solids: Role of the structural disjoining pressure. Curr Opin Colloid Interface Sci 2011;16:344–9.